

**High-current breakdown of the quantum Hall effect and electron heating in InSb/AlInSb**J. A. Alexander-Webber,<sup>1</sup> A. M. R. Baker,<sup>1</sup> P. D. Buckle,<sup>2</sup> T. Ashley,<sup>3</sup> and R. J. Nicholas<sup>1,\*</sup><sup>1</sup>*Department of Physics, Oxford University, Clarendon Laboratory, Parks Road, Oxford OX1 3PU, United Kingdom*<sup>2</sup>*School of Physics and Astronomy, Cardiff University, Queens' Building, The Parade, Cardiff CF24 3AA, United Kingdom*<sup>3</sup>*School of Engineering, University of Warwick, Coventry CV4 7AL, United Kingdom*

(Received 2 March 2012; revised manuscript received 24 May 2012; published 5 July 2012)

We report measurements of the temperature and electric field dependent breakdown of the quantum Hall effect in two-dimensional InSb/AlInSb heterostructures. The electron temperature  $T_e$  is studied as a function of electric field and it is shown that the energy loss rates of electrons to the lattice follow a  $(T_e^3 - T_L^3)$  dependence for  $2 \text{ K} < T_e < 22 \text{ K}$  at a lattice temperature  $T_L = 1.5 \text{ K}$ . The high-current induced breakdown of the quantum Hall effect (QHE) is linearly proportional to sample width as deduced from the Hall resistivity and shows breakdown at lower current densities as deduced from the resistivity ( $\rho_{xx}$ ) due to nonuniformity in carrier density. Temperature dependent studies show that the quantum Hall effect persists to considerably higher temperatures than the conventional GaAs/AlGaAs system. Using the energy loss rates, we describe the QHE breakdown in terms of bootstrap-type electron heating.

DOI: 10.1103/PhysRevB.86.045404

PACS number(s): 73.43.Qt, 72.20.Ht, 73.50.Fq

**I. INTRODUCTION**

The quantum Hall effect<sup>1</sup> (QHE), observed in two-dimensional electron gases (2DEGs) at low temperatures when a high magnetic field is applied perpendicular to the 2DEG plane, is characterized by a vanishing longitudinal resistivity  $\rho_{xx}$  and quantized Hall resistance  $\rho_{xy} = h/\nu e^2$ , where  $h$  is Planck's constant,  $e$  the electronic charge, and  $\nu$  the number of filled Landau levels. Since 1990 the QHE has been the electrical resistance unit standard, used to define the ohm, for which the persistence of the effect at high temperatures and electrical currents is of particular importance.<sup>2</sup> With increasing temperature a gradual increase of  $\rho_{xx}$  and deviation of  $\rho_{xy}$  from quantization is observed. With increasing current, however, a sudden transition occurs at critical current  $I_c$  at which point  $\rho_{xx}$  increases by several orders of magnitude. The breakdown of the QHE due to high currents has been studied extensively in semiconductor heterostructures (see Nachtwei<sup>3</sup> for a review) and more recently in graphene.<sup>4,5</sup> Breakdown phenomena are of particular interest due to their relevance in standards applications as well as the potential to elucidate the fundamental physics of the quantum Hall effect.

Indium antimonide has the narrowest band gap of any III-V semiconductor,<sup>6</sup> and even when confined to a 2DEG, electrons in InSb have been shown to have an effective mass of only  $m^* = 0.02m_e$  (Ref. 7) and an exceptionally large effective Landé  $g$  factor ( $g^* \sim -50$ ).<sup>8</sup> These properties lead to both large cyclotron energy ( $E_c = \hbar\omega_c = \hbar eB/m^*$ ) and large Zeeman ( $sg^*\mu_B B$ ) energy gaps, where  $\omega_c$  is the cyclotron frequency,  $B$  is the magnetic field,  $s = \pm 1/2$  is the spin of the electron, and  $\mu_B = \frac{eh}{2m_e}$  is the Bohr magneton. Using InSb heterostructures we have been able to study the effect of large energy gaps on the breakdown properties of the QHE.

**II. SAMPLE PROPERTIES**

All samples studied were InSb/Al<sub>x</sub>In<sub>1-x</sub>Sb heterostructures grown on a semi-insulating GaAs(001) substrate by solid-source molecular beam epitaxy.<sup>6</sup> The carriers are confined within a 30 nm InSb quantum well, between a 3  $\mu\text{m}$

Al<sub>0.10</sub>In<sub>0.90</sub>Sb buffer layer and a 50 nm upper barrier layer of Al<sub>0.15</sub>In<sub>0.85</sub>Sb containing a Te  $\delta$ -doping plane. The samples were fabricated into Hall bar geometries, of widths 75, 300, and 600  $\mu\text{m}$ , with wide current injection contacts at each end and three pairs of narrow voltage probes placed along the device (Fig. 1, inset). Carrier densities were in the range  $2\text{--}3.5 \times 10^{11} \text{ cm}^{-2}$  and mobilities exceed  $160\,000 \text{ cm}^2/\text{V s}$  at 1.5 K.

**III. ELECTRON HEATING AND ENERGY LOSS RATES**

Magnetotransport measurements were carried out using a superconducting solenoid magnet in a variable temperature insert with a base temperature of 1.5 K. A typical magnetotransport plot is shown in Fig. 1. Several well defined quantum Hall states are clearly observable. At lower fields the samples exhibit Shubnikov-de Haas (SdH) oscillations. At higher temperatures these oscillations are damped with the well known temperature dependence given by the Lifshitz-Kosevich formula

$$\frac{\Delta\rho}{\rho} = f(\omega_c) \frac{\chi}{\sinh(\chi)}, \quad (1)$$

with  $\chi = 2\pi^2 \frac{k_B T}{\hbar\omega_c}$ , where  $k_B$  is Boltzmann's constant and  $T$  is temperature, and  $\omega_c$  is the cyclotron frequency. When measured at low electric fields, electrons are at thermal equilibrium with the lattice and as such the thermal damping of the SdH oscillations is governed by the lattice temperature  $T_L$ . At high applied electric fields, however, carriers are unable to lose energy to the lattice through electron-phonon interactions at high enough rates and the two are no longer in thermal equilibrium. The electron temperature  $T_e$  increases relative to the lattice and the electrons collectively reach an internal thermal equilibrium due to electron-electron scattering. Shubnikov-de Haas oscillations of hot electrons are damped in the same way as with lattice temperature. Such oscillations may therefore be used as a measure of the hot electron temperature. Magnetotransport measurements at high lattice temperatures were taken and compared to the data with oscillations at high currents for several values of the occupancy

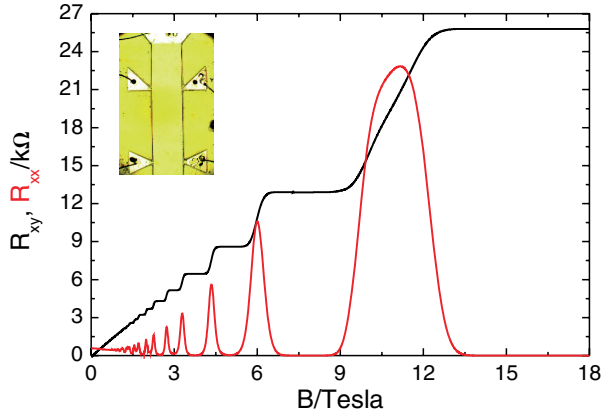


FIG. 1. (Color online) Resistivity plot showing the quantum Hall effect in InSb taken at 1.5 K using a current of 1  $\mu\text{A}$  with a sample carrier density of  $3.4 \times 10^{11} \text{ cm}^{-2}$ . Several well defined plateaus and minima for both even and odd integer filling factors are observed. Inset: A micrograph of a section of a typical 600  $\mu\text{m}$  wide eight-leg Hall bar.

$\nu$  to determine the electron temperature and to verify that Eq. (1) holds. As the current is increased above 1  $\mu\text{A}$  at 1.5 K, the electron temperature increases sublinearly to over 20 K with an applied current of 300  $\mu\text{A}$  at  $\nu = 4$  [Fig. 2(a)]. The total electrical power dissipated over the sample is measured for each occupancy. The energy loss rate per carrier  $P$  is thus calculated as a function of  $T_e$ . Empirically, we find

$$P = \alpha(T_e^3 - T_L^3), \quad (2)$$

with a value of  $\alpha = 8 \times 10^{-18} \text{ W K}^{-3}$ . A similar power law dependence following approximately  $P \propto T^3$  has been observed in this temperature regime in GaAs,<sup>10–13</sup> Si,<sup>14</sup> and SiGe,<sup>15,16</sup> as expected for a combination of deformation potential and piezoelectric scattering.<sup>13</sup> In the nonequilibrium regime the carriers lose energy to the lattice with a characteristic energy

relaxation time  $\tau_e$ . This is calculated, using

$$\tau_e = \frac{\pi^2 k_b^2 T_e^2}{3 E_F P} = \frac{\pi^2 k_b^2 T_e^2}{3 E_F \alpha (T_e^3 - T_L^3)}, \quad (3)$$

where  $E_F$  is the Fermi energy and  $n$  is the carrier density. Energy loss times at several filling factors are shown in Fig. 2(b) as a function of electron temperature. The energy loss times are slightly longer than values for GaAs taken from both electrical and optical measurements,<sup>9,10,17</sup> and significantly longer than found recently for graphene.<sup>5</sup>

#### IV. HIGH-CURRENT BREAKDOWN OF THE QUANTUM HALL EFFECT

The breakdown of the quantum Hall effect is characterized by a sudden increase from the zero resistivity state and a deviation from the quantized Hall resistance ( $\Delta\rho_{xy}$ ). We will define the point at which breakdown occurs as  $\rho_{xx}$  or  $\Delta\rho_{xy} \gtrsim 1 \Omega$ . High-current breakdown is observed by measuring the  $I$ - $V_{xx}$  characteristics of the sample in a four-terminal configuration. A series of such  $I$ - $V_{xx}$  traces are shown in Fig. 3 for a 600  $\mu\text{m}$  wide Hall bar at 1.5 K. Clear quantum Hall breakdown is observed for both  $\nu = 1$  and  $\nu = 2$  as a sudden onset of dissipation. We find critical current values for the two filling factors of  $I_c(\nu = 1) = 145 \mu\text{A}$  and  $I_c(\nu = 2) = 180 \mu\text{A}$  [Fig. 3(b)].

By contrast the deviation from quantization of the Hall resistance within the plateau shows a sudden deviation at currents much greater than that of  $I_c$  [Fig. 3(c)]. Previous investigations of the dependence of  $\Delta\rho_{xy}$  on  $\rho_{xx}$  have shown two different types of phenomena. The first was a linear relationship due to thermal activation, where  $\Delta\rho_{xy} = S\rho_{xx}$ .<sup>18,19</sup> The second showed an abrupt drop of a few ppm from quantization at currents of  $\approx 0.8I_c$ ,<sup>20</sup> ascribed to delocalization of electrons and not thermal activation. Our observations clearly differ from both of these but have more in common with the abrupt

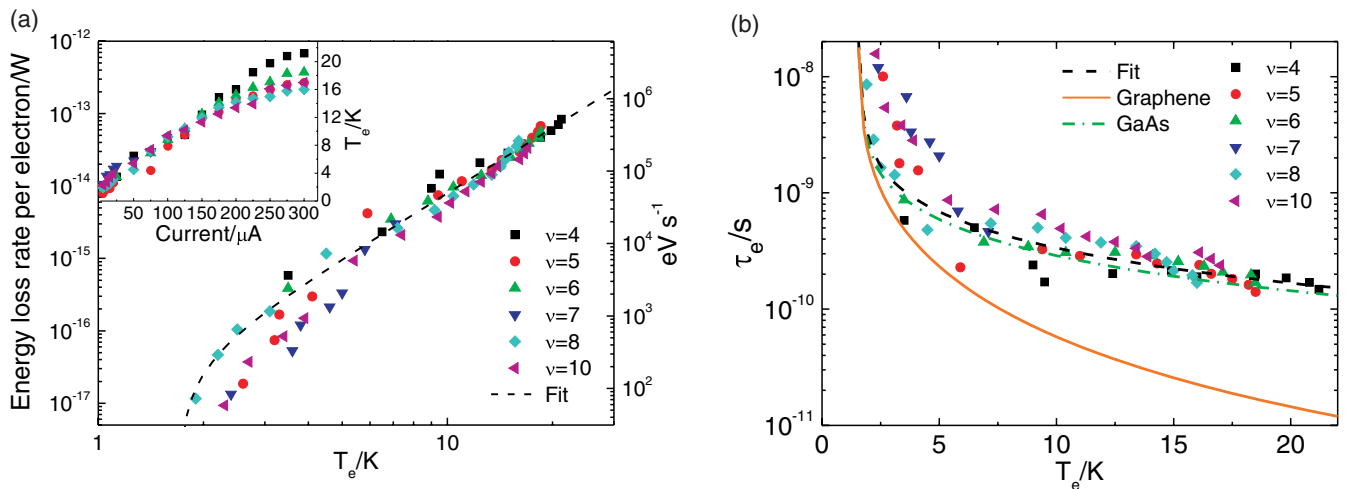


FIG. 2. (Color online) (a) Energy loss rates as a function of electron temperature measured at a fixed  $T_L = 1.5 \text{ K}$  for a sample with a carrier density of  $2.55 \times 10^{11} \text{ cm}^{-2}$ . The rate follows the expected  $(T_e^3 - T_L^3)$  dependence. Electron temperature is measured as a function of current as shown in the inset. (b) Relaxation time as a function of electron temperature as deduced from Eq. (3). Also shown is  $\tau_e$  for graphene (Ref. 5) and GaAs at 1.5 K, as deduced from optical (Ref. 17) and electrical (Refs. 9 and 10) measurements of energy loss rate as a function of electron temperature.

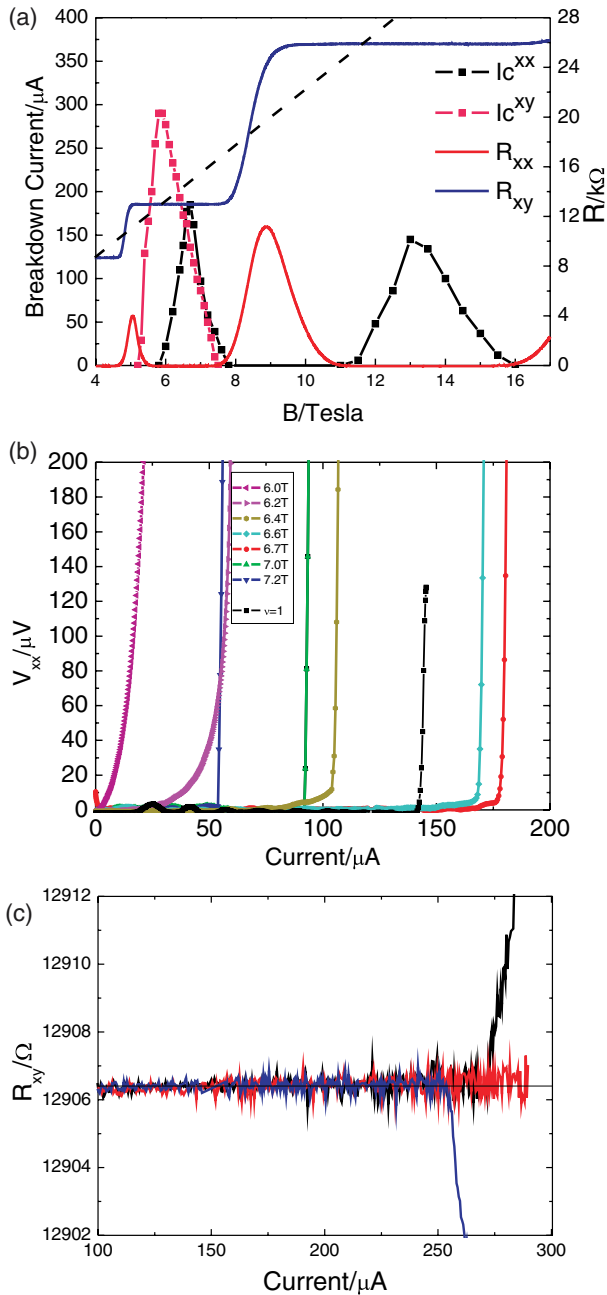


FIG. 3. (Color online) (a) Field dependence of breakdown currents for a  $600\ \mu\text{m}$  device with carrier density of  $3.3 \times 10^{11}\ \text{cm}^{-2}$  shown with the magnetotransport plot. The dashed black line indicates the predicted conventional Hall resistance which crosses the Hall plateau at integer filling factors. (b) The current voltage characteristics for  $\nu = 2$  (colors) and  $\nu = 1$  (black) clearly showing a sudden onset of resistance following a critical current. At magnetic fields below the field of highest breakdown current, the longitudinal voltage dropped is a more gradual increase with increasing current. Above this field a more sudden, steplike increase is observed indicating a different type of phase transition. (c) The deviation of the Hall voltage from quantized values at  $\nu = 2$  for three magnetic field values corresponding to  $\nu = 1.965$  (blue),  $\nu = 2$  (red), and  $\nu = 2.07$  (black).

deviation as seen by Kawashima *et al.* as we do not see a linear relationship within the noise levels of a few ppm.

The magnetic field dependence of the breakdown current is shown in Fig. 3(a). Due to the macroscopic scale of the sample there are significant inhomogeneities leading to a significant difference in the magnetic field at which the current occupancy occurs, and this will be greatest in the current direction due to the larger physical separation of the  $V_{xx}$  contacts. A comparison of the magnetic field dependence of the breakdowns of  $\rho_{xx}$  and the Hall deviation for  $\rho_{xy}$  suggest that inhomogeneities in the carrier density probably play a significant role in the behavior observed. On the high field side of the plateau the breakdown current is very similar for  $\rho_{xx}$  and  $\rho_{xy}$  [Fig. 3(a)]. At the same time the nature of the breakdown is the well known abrupt breakdown with a sudden onset of resistance. By contrast, at lower fields where the  $\rho_{xy}$  quantum Hall current gives considerably larger breakdown values than observed for  $\rho_{xx}$ , the resistivity  $\rho_{xx}$  shows a gradual onset [Fig. 3(b)]. This is consistent with multiple successive breakdowns in regions of progressively increasing carrier density which reach the breakdown condition at lower fields. Further evidence for this comes from measuring the outer contacts which have twice the separation and show a further decrease in the breakdown current. The  $\rho_{xy}$  breakdown current is a maximum, as expected, where the  $\nu = 2$  state is at exact integer occupancy as calculated from the classical Hall coefficient measured at high temperature, whereas the  $\rho_{xx}$  minima are at slightly higher fields and are centered on the peak breakdown current for  $\rho_{xx}$ .

Using three  $600\ \mu\text{m}$  wide Hall bars with carrier densities of  $1.3 \times 10^{11}\ \text{cm}^{-2}$ ,  $2.3 \times 10^{11}\ \text{cm}^{-2}$ , and  $3.3 \times 10^{11}\ \text{cm}^{-2}$ , we have studied the field dependence of the peak breakdown current at  $\nu = 1$  and 2 [Fig. 4(a)]. We find a linear dependence of  $\nu = 1$  breakdown current with magnetic field. The data for  $\nu = 2$  are also consistent with a linear increase with magnetic field, with the exception of the lowest density sample which does not have sufficiently well resolved oscillations to give quantum Hall behavior.

One issue encountered was a runaway increase in contact resistance at high currents and high magnetic fields. From two contact measurements it was found that at high fields the voltage dropped at the contacts becomes several times that of the Hall voltage. Due to this effect increasing with magnetic field, this meant that we were only able to probe the peak Hall deviation current for  $\nu = 2$  and not  $\nu = 1$ .

### A. Geometric dependence

A number of studies on low mobility samples have shown that the critical breakdown current scales linearly with the Hall bar width,<sup>21</sup> consistent with the existence of a critical electric field for the breakdown of the quantum Hall effect. Critical currents in high mobility samples, on the other hand, have been shown to increase sublinearly with width.<sup>22</sup> This leads to the breakdown condition being described as a critical current density, ranging from  $\sim 0.1$  to  $1.6\ \text{A/m}$  (Refs. 21 and 22) in GaAs and recently up to  $8\ \text{A/m}$  in exfoliated graphene<sup>5</sup> and  $14.3\ \text{A/m}$  in polymer gated epitaxial graphene.<sup>4</sup>

We have studied the width dependence of  $I_c$  in devices of three widths,  $75$ ,  $300$ , and  $600\ \mu\text{m}$ , all with equal aspect ratios. Figure 4(b) shows that there is a linear dependence of the current for the onset of quantum Hall deviation ( $\Delta\rho_{xy}$ )

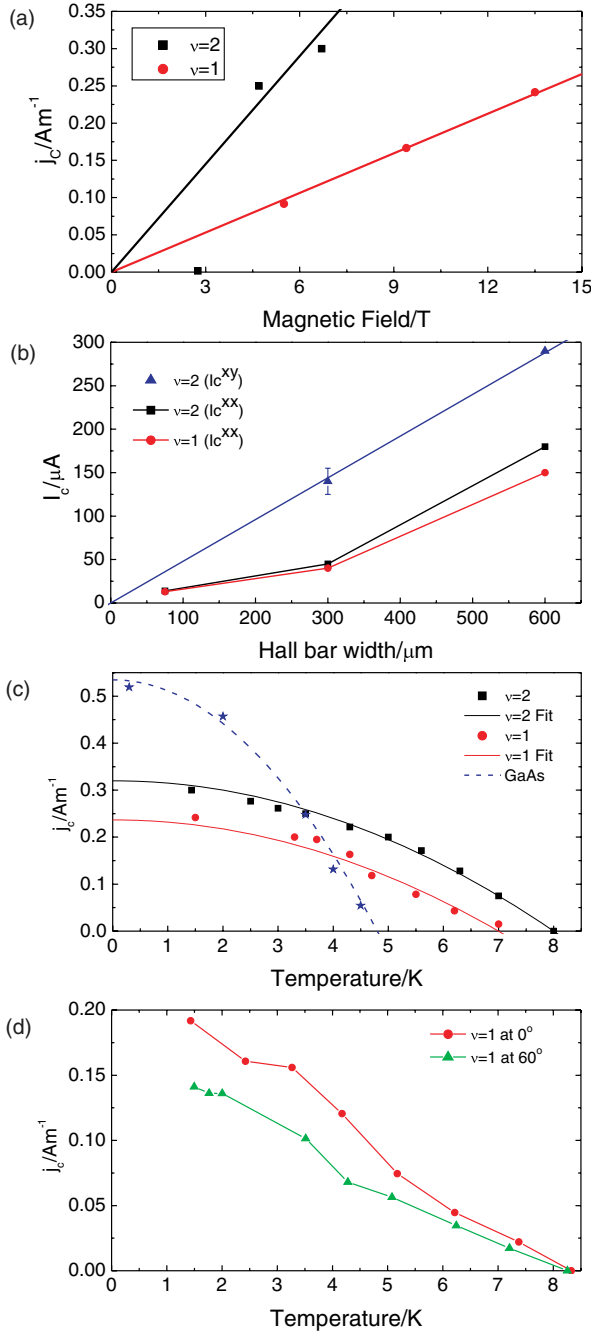


FIG. 4. (Color online) (a) The magnetic field dependence of peak breakdown current density for  $\nu = 2$  (black) and  $\nu = 1$  (red) from three  $600 \mu\text{m}$  Hall bars with carrier densities of  $1.3 \times 10^{11} \text{ cm}^{-2}$ ,  $2.3 \times 10^{11} \text{ cm}^{-2}$ , and  $3.3 \times 10^{11} \text{ cm}^{-2}$ . At the lowest carrier density the  $\nu = 2$  state is not well defined with  $I_c \sim 1 \mu\text{A}$ . (b) Width dependence of maximum Hall deviation current for  $\nu = 2$  (blue) and  $I_c$  for  $\nu = 2$  (black) and  $\nu = 1$  (red). The three widths used were  $75$ ,  $300$ , and  $600 \mu\text{m}$ . (c) Temperature dependence of longitudinal breakdown current density for  $\nu = 2$  ( $6.1 \text{ T}$ , black) and  $\nu = 1$  ( $12.2 \text{ T}$ , red) for a  $600 \mu\text{m}$  Hall bar fitted using Eq. (4). Also shown for comparison is the temperature dependence of  $\nu = 2$  in GaAs at  $4.8 \text{ T}$  (blue dashed) taken from Ref. 23. (d) Temperature dependence of breakdown current density for  $\nu = 1$  perpendicular to the magnetic field ( $9 \text{ T}$ ) and at  $60^\circ$  ( $18 \text{ T}$ ), taken with a  $75 \mu\text{m}$  device.

giving a critical current density of  $0.5 \text{ A/m}$ . A study of  $I_c$  from the breakdown of  $\rho_{xx}$  shows lower values than observed from  $\Delta\rho_{xy}$ , and considerably more variability and dependence on contact arrangements which we attribute to both macroscopic and microscopic inhomogeneities in electron density, as discussed above.

### B. Temperature dependence

Indium antimonide quantum Hall resistance standards would offer a distinct advantage over conventional GaAs devices if they could be operated at higher temperatures. To study this, the field was set at the position of maximum breakdown current and the temperature varied. The temperature dependences of the longitudinal  $\rho_{xx}$  breakdown current for both  $\nu = 1$  and  $\nu = 2$  in a  $600 \mu\text{m}$  Hall bar were studied [Fig. 4(c)]. Both plateaus are seen to show very little reduction in breakdown current to well above the helium-4 temperature of  $4.2 \text{ K}$ . This compares well to the equivalent temperature dependence observed for GaAs devices. Typical results for a similar GaAs sample<sup>23</sup> with a carrier density of  $2.4 \times 10^{11} \text{ cm}^{-2}$  are also shown in Fig. 4(c) for comparison. While GaAs may have higher critical current densities at low temperatures, the breakdown current for the QHE falls much faster with increasing temperature. This means that at  $4.2 \text{ K}$ , the breakdown current of GaAs is only  $\sim 20\%$  of its low temperature value, whereas for InSb the breakdown current remains at over  $85\%$ . We can approximate the temperature dependence<sup>23</sup> of the quantum Hall breakdown current density  $j_c$  using

$$j_c = j_c^0 \left( 1 - \frac{T_c^2}{T^2} \right), \quad (4)$$

where  $j_c^0$  is the breakdown current density at zero temperature and  $T_c$  is the critical temperature, above which QHE is not observed. We find that while the absolute breakdown current density is higher in GaAs, the critical temperature is higher in InSb with  $T_c \approx 8 \text{ K}$  due to the larger Landau and spin-split energy gaps. In GaAs the value of  $T_c$  has been found to scale with magnetic field at almost exactly  $1 \text{ K/T}$ .<sup>24</sup> Assuming the same behavior for InSb based on the results for the linear field scaling of  $j_c^0$  [Fig. 4(a)] would suggest a value of  $\approx 1.3 \text{ K/T}$ , which is significantly larger than for GaAs but is not scaling linearly with the magnitude of the cyclotron energy.

The most widely accepted theory of the breakdown of the QHE has been described in the work of Komiyama and Kawaguchi and is based on bootstrap-type electron heating.<sup>25,26</sup> It predicts that breakdown occurs at a critical electric field  $E_c$ , which is determined by the energy relaxation time given by

$$E_c = \sqrt{\frac{4B\hbar\omega_c}{2e\tau_e}}, \quad (5)$$

assuming a twofold (spin) degeneracy of the Landau levels. This yields a predicted critical electric field of  $27.1 \text{ kV/m}$  at  $6 \text{ T}$  using  $\tau_e = 500 \text{ ps}$ , the value at the breakdown temperature of  $8 \text{ K}$ . This corresponds to a  $\nu = 2$  breakdown current density of  $2.1 \text{ A/m}$ , compared to the experimental value of  $0.5 \text{ A/m}$

observed for the  $\rho_{xy}$  deviation. This difference is not surprising as the theory is known to overestimate  $E_c$  by a factor of 2–4 when compared to the highest values observed in even the most well optimized wide Hall bars in GaAs.<sup>21</sup> This is probably due to uncertainties in the most appropriate value of  $\tau_e$  which should be used.

### C. Breakdown of spin-split quantum Hall states

The temperature dependence of the breakdown current for  $\nu = 1$  was also studied in a  $75 \mu\text{m}$  device as shown in Fig. 4(d). InSb is very different from GaAs due to the very high electron  $g$  factor, which means that large quantum Hall breakdown currents can also be observed at high temperatures for  $\nu = 1$ , where the separation between the two spin levels is comparable to the Landau splitting for  $\nu = 2$ . The breakdown currents for  $\nu = 1$  are only slightly smaller than for  $\nu = 2$ , which means that  $E_c(\nu = 1)$ , is significantly ( $\sim 60\%$ ) higher than for  $\nu = 2$  and the quantum Hall effect persists up to similar temperatures. In GaAs at low temperatures ( $< 0.5$  K) in a given sample,  $E_c(\nu = 1)$  is found to be equivalent to  $E_c(\nu = 2)$ .<sup>27</sup>

The spin splitting is known to be significantly enhanced by rotating the sample relative to the magnetic field direction.<sup>8</sup> Figure 4(c) shows a comparison for two measurements with the same perpendicular field for a narrow channel sample ( $75 \mu\text{m}$ ) with the sample at  $0^\circ$  and  $60^\circ$  to the applied field, i.e., a doubling in the total magnetic field. While the spin

splitting increases between  $0^\circ$  and  $60^\circ$  by a factor close to 2, the breakdown current actually falls. We attribute this to a mixing of energy levels in the quantum well, which leads to additional breakdown possibly due to coupling to bulk and higher energy states.

### V. SUMMARY

We have observed quantum Hall effect in the narrow band-gap InSb/AlInSb system. We have shown that the large cyclotron energy leads to the quantum Hall effect persisting to higher temperatures than seen for GaAs, although the maximum value of the critical current is somewhat smaller due to the lower energy loss rate. We have shown that the high-current breakdown can be observed for of spin-polarized quantum Hall states at  $\nu = 1$ , and that the critical breakdown field is higher than that at  $\nu = 2$ . Deviation from Hall quantization at high electric fields is abrupt and is shown to occur at currents much greater than those required to see longitudinal dissipation, which is related to the presence of significant sample density inhomogeneities.

### ACKNOWLEDGMENTS

We thank M. T. Emeny and L. Buckle for providing the samples. This work was supported by EPSRC.

\*r.nicholas1@physics.ox.ac.uk

<sup>1</sup>K. V. Klitzing, G. Dorda, and M. Pepper, *Phys. Rev. Lett.* **45**, 494 (1980).

<sup>2</sup>B. Jeckelmann and B. Jeanneret, *Rep. Prog. Phys.* **64**, 1603 (2001).

<sup>3</sup>G. Nachtwei, *Physica E* **4**, 79 (1999).

<sup>4</sup>T. J. B. M. Janssen, A. Tzalenchuk, R. Yakimova, S. Kubatkin, S. Lara-Avila, S. Kopylov, and V. I. Fal'ko, *Phys. Rev. B* **83**, 233402 (2011).

<sup>5</sup>A. M. R. Baker, J. A. Alexander-Webber, T. Altbauer, and R. J. Nicholas, *Phys. Rev. B* **85**, 115403 (2012).

<sup>6</sup>J. M. S. Orr, A. M. Gilbertson, M. Fearn, O. W. Croad, C. J. Storey, L. Buckle, M. T. Emeny, P. D. Buckle, and T. Ashley, *Phys. Rev. B* **77**, 165334 (2008).

<sup>7</sup>J. M. S. Orr, K.-C. Chuang, R. J. Nicholas, L. Buckle, M. T. Emeny, and P. D. Buckle, *Phys. Rev. B* **79**, 235302 (2009).

<sup>8</sup>B. Nedniyom, R. J. Nicholas, M. T. Emeny, L. Buckle, A. M. Gilbertson, P. D. Buckle, and T. Ashley, *Phys. Rev. B* **80**, 125328 (2009).

<sup>9</sup>Y. Ma, R. Fletcher, E. Zaremba, M. DiIorio, C. T. Foxon, and J. J. Harris, *Phys. Rev. B* **43**, 9033 (1991).

<sup>10</sup>D. R. Leadley, R. J. Nicholas, J. J. Harris, and C. T. Foxon, *Semicond. Sci. Technol.* **4**, 879 (1989).

<sup>11</sup>S. J. Manion, M. Artaki, M. A. Emanuel, J. J. Coleman, and K. Hess, *Phys. Rev. B* **35**, 9203 (1987).

<sup>12</sup>J. Shah, A. Pinczuk, A. C. Gossard, and W. Wiegmann, *Phys. Rev. Lett.* **54**, 2045 (1985).

<sup>13</sup>M. E. Daniels, B. K. Ridley, and M. Emeny, *Solid-State Electron.* **32**, 1207 (1989).

<sup>14</sup>R. Fletcher, V. M. Pudalov, Y. Feng, M. Tsaousidou, and P. N. Butcher, *Phys. Rev. B* **56**, 12422 (1997).

<sup>15</sup>G. Stöger, G. Brunthaler, G. Bauer, K. Ismail, B. S. Meyerson, J. Lutz, and F. Kuchar, *Phys. Rev. B* **49**, 10417 (1994).

<sup>16</sup>R. Leturcq, D. L'Hôte, R. Tourbot, V. Senz, U. Gennser, T. Ihn, K. Ensslin, G. Dehlinger, and D. Grützmacher, *Europhys. Lett.* **61**, 499 (2003).

<sup>17</sup>K. Leo, W. W. Ruhle, and K. Ploog, *Phys. Rev. B* **38**, 1947 (1988).

<sup>18</sup>K. Yoshihiro, J. Kinoshita, K. Inagaki, C. Yamanouchi, J. Moriyama, and S. Kawaji, *Physica B + C* **117-118**, 706 (1983).

<sup>19</sup>M. E. Cage, B. F. Field, R. F. Dziuba, S. M. Girvin, A. C. Gossard, and D. C. Tsui, *Phys. Rev. B* **30**, 2286 (1984).

<sup>20</sup>H. Kawashima, H. Tanaka, and S. Kawaji, *J. Phys. Soc. Jpn.* **74**, 2791 (2005).

<sup>21</sup>S. Kawaji, K. Hirakawa, and M. Nagata, *Physica B* **184**, 17 (1993).

<sup>22</sup>N. Q. Balaban, U. Meirav, H. Shtrikman, and Y. Levinson, *Phys. Rev. Lett.* **71**, 1443 (1993).

<sup>23</sup>H. Tanaka, H. Kawashima, H. Iizuka, H. Fukuda, and S. Kawaji, *J. Phys. Soc. Jpn.* **75**, 1 (2006).

<sup>24</sup>L. B. Rigal, D. K. Maude, M. Potemski, J. C. Portal, L. Eaves, J. R. Wasilewski, G. Hill, and M. A. Pate, *Phys. Rev. Lett.* **82**, 1249 (1999).

<sup>25</sup>S. Komiyama, Y. Kawaguchi, T. Osada, and Y. Shiraki, *Phys. Rev. Lett.* **77**, 558 (1996).

<sup>26</sup>S. Komiyama, T. Takamasu, S. Hiyamizu, and S. Sasa, *Solid State Commun.* **54**, 479 (1985).

<sup>27</sup>S. Kawaji, *Semicond. Sci. Technol.* **11**, 1546 (1996).